Advanced and Sustainable Technologies
ASET
E-ISSN 2976-2294
Volume 4, No 2, December 2025 [1-25]

Modelling the Selective Recovery of Praseodymium, Neodymium, Terbium, and Dysprosium from Malaysian Saprolite Using a Multi-Extraction System

Farouq Ahmat[1*] and Mohd Yusri Mohd Yunus[1]

[1]Faculty of Chemical and Natural Resources Engineering, Universiti Malaysia Pahang Al-Sultan Abdullah, Lebuhraya Tun Razak, 26300 Gambang, Kuantan, Pahang, Malaysia.

Received 24 April 2025, Revised 21 May 2025, Accepted 25 June 2025

ABSTRACT

The extraction of rare earth elements is complex, arduous, and laborious because of the similarity of the physicochemical properties of adjacent elements. The introduction of cascade solvent extraction allows for the simultaneous extraction of rare earth elements with high purity and recovery. However, no single extractant is capable of effectively extracting all the rare earth elements; hence, multiple extractants are required to extract the target elements. This present study describes the model for extracting rare earth by integrating hexylphosphic mono-2-ethylhexyl ester and Di-(2-ethylhexyl) phosphoric acid with hydrochloric acid as the scrubbing agent in a kerosene medium, as an extensive extraction was introduced. However, the lack of an efficient and structured framework for executing the extensive integration of a multi-extraction system presents a significant challenge. Currently, there is no established systematic framework for integrating multiple extractants to facilitate the separation of rare earth elements. In response, a systematic extraction framework was developed and used to model this extensive extraction method. The ultimate purpose of the model was to accurately predict the separation stage at equilibrium, as well as its outcomes, and to evaluate the effects of the feed ratio, reflux of extraction and scrubbing, and mass flow rate on the separation stage. It was found that the optimal ratio of the easily extractable solute to the more difficult solute, as well as the ratio of extraction to scrubbing reflux through modeling, was 50:50. The extraction process required 379 stages to achieve approximately 99.99% purity and 99.0% recovery of praseodymium, neodymium, terbium, and dysprosium from saprolite. The amount of extracted praseodymium, neodymium, terbium, and dysprosium can reach 55.74 tons per annum by adopting the proposed multi-extraction system.

Keywords: Extraction framework, Reflux, Solvent extraction, Separation factor, Xu counter-current principle.

1. INTRODUCTION

The extraction of rare earth elements (REEs) is challenging because of the similarity in the physicochemical properties of adjacent elements. The extraction process aimed at recovering individual REEs from the primary source is complex and laborious. The extraction of REEs is commonly carried out using the solvent extraction (SX) method because of its simplicity. This method is based on two immiscible liquids, whereby the lighter organic phase floats on the heavier aqueous phase, and the extraction is relatively fast, which can be performed continuously. The extraction of REEs by SX requires multi-stage recovery, known as cascade SX. Cascade SX requires a suitable extractant, such as phosphonic acid, phosphoric acid, naphthenic acid, or the Cyanex series of extractants, to perform the extraction. These extractants are commonly known

*Corresponding author: farouq_ahmat@yahoo.com

by their commercial names, such as P204, P507, P350, C272, and C923. However, a single extraction system is incapable of recovering all individual elements. Therefore, integrating multiple extraction systems into an extensive recovery system is essential. The recovery process is immense, sophisticated, and tedious when involving a multi-extraction system.

The unavailability of a framework for carrying out the massive integration of a multi-extraction system poses a significant challenge. Hence, in order to address this, the present study builds upon the foundational work of Xu Guangxian, particularly his cascade counter-current extraction principle [1,2]. The conceptual foundation of this study adheres to the pioneering work of Xu Guangxian, who developed the cascade theory for rare earth element separation. His work introduced a rigorous stage-by-stage modelling approach for SX processes, focusing on equilibrium conditions and the relationship between separation factors across cascades. Xu's theory remains fundamental to calculating the number of stages required to achieve a desired purity and recovery in REE separation. This present study expanded Xu's theory when developing this framework to accommodate multi-extractant systems and enabling the modelling of multiple extraction circuits tailored to specific REEs, such as neodymium (Nd), praseodymium (Pr), terbium (Tb), and dysprosium (Dy). This extension provides a more flexible and application-oriented process design, particularly suited to complex feedstocks, like Malaysian saprolite.

The proposed multi-extraction system comprising P507-HCl and P204-HCl extraction systems in kerosene media was used to model the extraction of Nd, Pr, Tb, and Dy from Malaysian saprolite. Malaysia has an estimated 30,000–43,000 tons of untapped REE reserves, and these elements are commonly associated with the by-products of tin mining and ion-adsorption clay [3–5]. Saprolite is a potentially untapped rare earth resource in Malaysia. The Malaysian saprolite layer is clay associated with rich REEs and has no radioactive elements. Comparatively, their concentration is at par with other major minerals, such as Iron Hill Colorado Carbonatite and Canada Nechalacho ore, as shown in Figure 1 [4, 6–8].

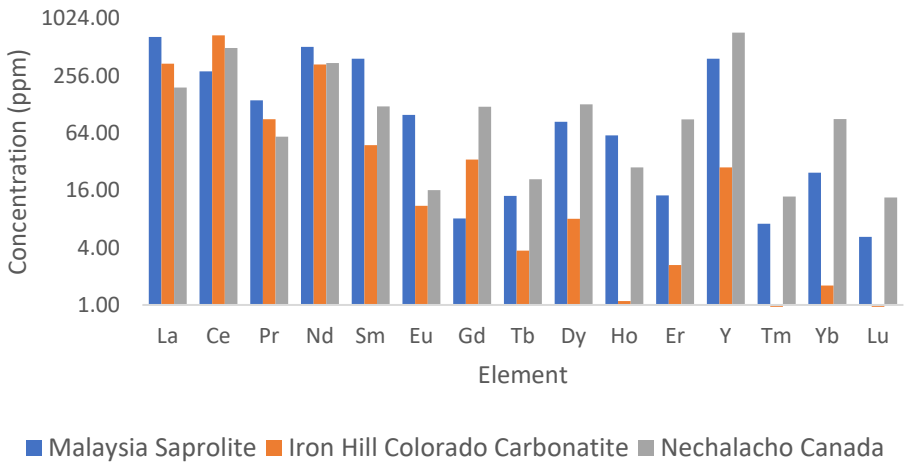

Figure 1: REE distribution in Malaysia saprolite, Nechalacho ore, and Iron Hill Colorado carbonatite.

SX is commonly used to extract these elements because of its ability to simultaneously achieve high purity, recovery, and yield [1,2]. The SX process can be divided into three steps, namely extraction, scrubbing, and stripping. The extractant is used as an organic solution for solvent extraction. Many types of extractants are commercially available for REE extraction, but the application depends on the suitability of the extractant. REEs can be classified into three groups based on their extractability, such as light rare earth elements (LREEs), middle rare earth elements (MREEs), and heavy rare earth elements (HREEs). The 2-ethyl hexylphosphic mono-2-ethylhexyl ester (P507) effectively recovered individual HREEs, such as Tb and Dy. Nd and Pr,

which were extracted using di-(2-ethylhexyl) phosphoric acid (P204). The advantages of P507 and P204 over other extractants are their low cost, high loading capacity, and high selectivity of REEs. One setback of using P507 and P204 is the tendency to form a gel-like emulsion during extraction. The assessment method used for selecting the ideal method to extract REEs is discussed thoroughly in this study. This study presents an in-depth examination of a model for extracting Nd, Pr, Tb, and Dy using a multi-stage extraction system based on P507-HCl and P204-HCl in a kerosene medium, approached from a fundamental process perspective. The approach developed in this study offers a clearer understanding of how different factors interact in complex cascade REE extraction systems. The model helps identify optimal conditions for improved performance by modelling the process under various operating conditions, such as phase ratios, separation factors, and reflux flows. This enables a more precise control over the extraction and scrubbing stages. In doing so, the methodology supports the design for more reliable, cost-effective, and sustainable REE extraction processes suitable for industrial-scale implementation.

2. MODELLING

2.1 Basis of modelling

Multi-extraction systems, designed by integrating the P507 and P204 extraction systems into an extensive extraction process, were used to recover Nd, Pr, Tb, and Dy from saprolite. This study did not employ a saponification process for the extraction systems. The extraction system was selected based on five prominent extractant attributes: selectivity, tendency to form an emulsion, loading capacity, cost, and toxicity. The extraction circuit for each element was determined based on the average and adjacent separation factors. A large REE spectrum disintegrates into smaller groups and finally into individual elements. REEs are easier to extract by first disintegrating them into small groups according to their atomic number, which indicates their similarity in physicochemical properties. The SX configurations used in this process modelling were cascade fractional and counter-current SX, with the former applied to the extraction and scrubbing processes, while the latter was applied to the stripping process.

2.2 The proposed separation flowsheet

A P507 extraction system was initially used to divide the REE spectrum into LREEs and a mixture of MREEs and HREEs. Then, MREEs were extracted from the HREEs using the same system, and subsequently, P204 was used to extract the LREEs. The proposed separation flowsheet for recovering Nd, Pr, Tb, and Dy from saprolite is shown in Table 1 and Figure 2, respectively.

Table 1: Nd, Pr, Tb, and Dy extraction steps.

Circuit	Separation circuit	Category	Extractant	Scrubbing	Stripping
1	LREEs/MREEs+HREEs	Intermediate extraction	P507	HCl	HCl (LREEs)
1(a)	LaCe/NdPr*	Intermediate extraction	P204	HCl	Not required
1(b)	Pr/Nd	Individual extraction	P204	HCl	HCl (Nd)
2	MREEs/HREEs	Intermediate extraction	P507	HCl	HCl (MREEs)
3	TbDyHoEr/TmYbLuY*	Intermediate extraction	P507	HCl	Not required
3(a)	TbDy/HoEr*	Intermediate extraction	P507	HCl	Not required
3(b)	Tb/Dy	Individual extraction	P507	HCl	HNO_3 (Dy)

* Stripping is not required for this circuit

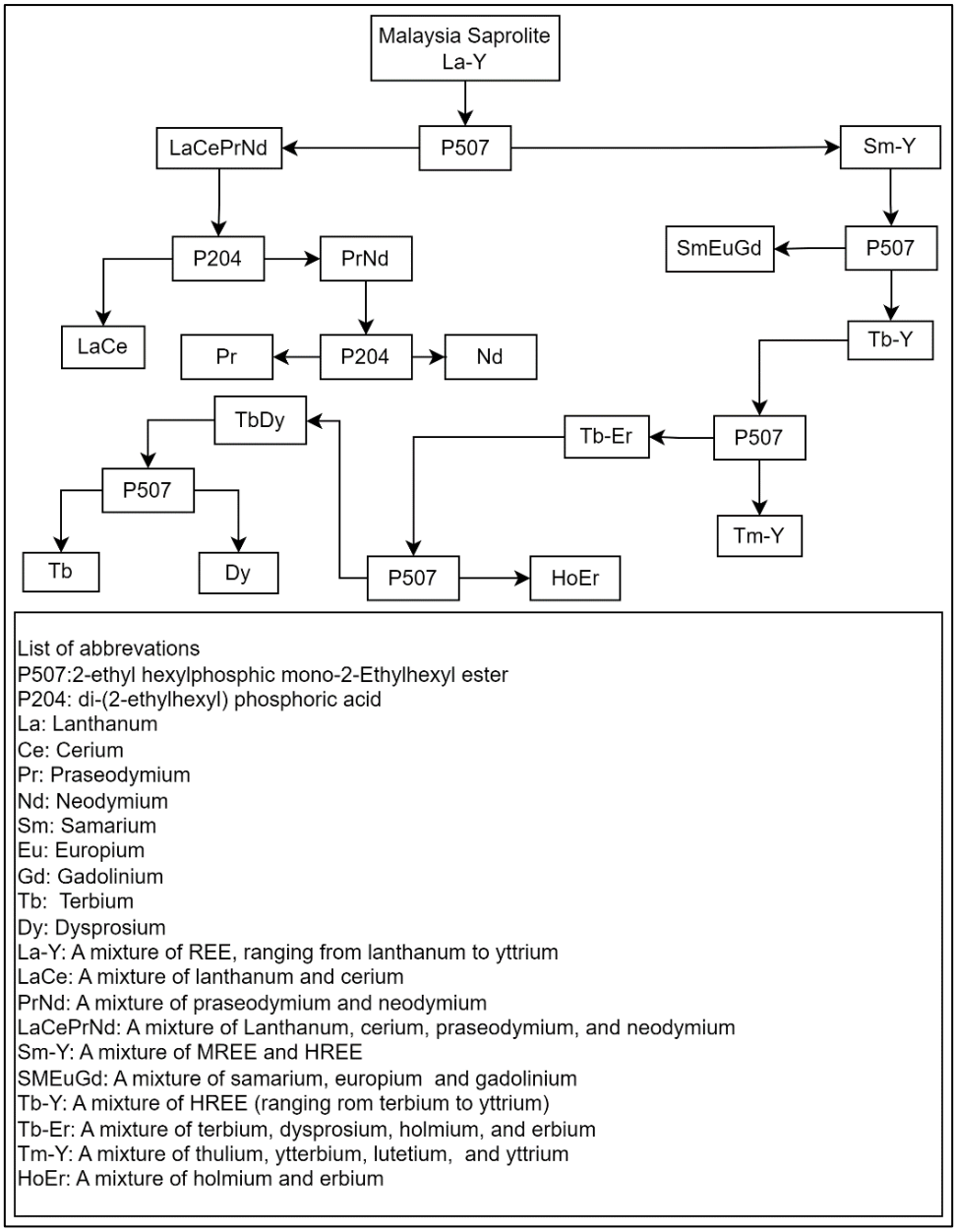

Figure 2: The proposed process flowsheet for recovering Nd, Pr, Tb, and Dy.

2.2.1 Extraction of light rare earth elements and heavy rare earth elements

Initially, REEs were introduced into the system in the aqueous phase, and the LREEs, which were prepared for individual extraction, were then extracted and separated from the MREEs and HREEs using P507. In the subsequent extraction stage, P507 was employed again to separate the HREEs from the MREEs, creating a distinct cutline. The rationale behind this 'cutline approach', which divides the REEs into LREEs, MREEs, and HREEs, is to streamline the separation process and enhance separation efficiency in the circuit.

2.2.2 Extraction of neodymium and praseodymium

The process began by stripping LREEs from P507 using 3.0 mol HCl. Subsequently, P204 was used to extract Nd and Pr from the LREEs group. Initially, LaCeNdPr was split into two intermediate groups, namely LaCe and NdPr. Subsequently, Nd and Pr were individually recovered from NdPr, with Nd being stripped from the aqueous phase through the application of 3.0 mol HCl.

2.2.3 Extraction of terbium and dysprosium

HREEs must be subdivided into more manageable groups in order to extract Tb and Dy. Initially, the HREEs group included Tb, Dy, Ho, Er, Tm, Yb, Lu, and Y. The initial step is to split this larger group into two smaller groups, as in TbDyHoEr and TmYbLuY. Subsequently, TbDy was separated from HoEr, and Tb was extracted from Dy. Dy was stripped from the organic phase using 0.1 M HNO_3.

2.3 Methodology framework

Process modelling was performed to extract Nd, Pr, Tb, and Dy from the saprolite. The flowchart (see Figure 3) summarizes the overall methodology framework of the process modelling. The framework was meticulously crafted as a step-by-step methodology for designing the extraction process, starting from sampling and culminating in the acquisition of individual REEs. The flowchart presents a clear and structured approach for designing and evaluating the REE extraction and separation process. It starts with characterizing the feed material in order to understand its composition, followed by selecting the specific element for recovering and choosing a suitable extraction system. A key decision point is whether the metal complexes formed can be easily stripped, and if not, the extraction system needs to be reconsidered. Thus, if stripping is feasible, the process moves on to selecting the stripping method and determining the separation factor and circuit. The separation's feasibility is then assessed, and if it is not viable, adjustments are made. Elements are grouped based on how easily they can be extracted, and their target purity, recovery, and concentration are set. The process checks whether the mass balance is satisfied, and if not, earlier steps are revisited. Once the mass balance is confirmed, the expected production output is compared against the target. After that, the mass balance table is constructed, flow ratios are calculated, and the number of separation stages is determined. Finally, process variables are optimized, and a comprehensive evaluation is carried out to ensure the process is technically sound and economically viable.

Several assumptions must be made to ensure that the framework is feasible. These assumptions are made according to the Xu cascade counter-current principle. The assumptions established during the process modelling were that the extraction and scrubbing stages are in equilibrium, and all H^+ ions in the starting scrubbing stage are assumed to be immediately exchanged and migrated toward the organic phase after entering the cascade SX. This implies that proton transfer kinetics are sufficiently fast and equilibrium is reached in each stage. This assumption is generally valid under well-controlled laboratory or design conditions, where adequate residence time and mixing are present. However, in real-world operations, deviations from this ideal behaviour can occur due to factors such as incomplete mixing, mass transfer limitations or variations in acidity and phase ratios. These non-idealities can lead to partial proton exchange that ultimately reduces scrubbing efficiency. Nevertheless, the assumption offers a practical simplification that supports tractable and efficient process design calculations. Aqueous and organic components had the same mixed extraction factor, and the phase ratio (*R)* was constant throughout the extraction (n) and scrubbing (m) stages except for the 1, n-1, n, n+1, and n+m stages. The separation factor ($\beta_{Z+1/Z}$)) was assumed to be constant in each stage throughout the separation circuit. In an actual circuit, adjacent separation factor ($\beta_{Z+1/Z}$) variation occurs in each stage, but the variation is small and negligible [1,2]. Although in reality, separation factors can change with solute concentration and phase ratio, it is worth noting that only a small portion of the total solute in each stage in the circuit process experiences this. This means that the concentrations in the feed and raffinate streams entering and leaving each stage are nearly the same. The separation factor stays nearly constant across the stages because the distribution coefficient (D), and thus $\beta_{Z+1/Z}$, is only slightly affected by such small concentration differences. In addition, the separation factor ($\beta_{Z+1/Z}$) in the extraction stage was assumed to have the same value as that in the scrubbing stage ($\beta'_{Z+1/Z}$)). It was assumed that each stage had equal holdup volumes for the aqueous and organic phases. All assumptions were consistent with the Xu cascade

counter-current principle [1,2].

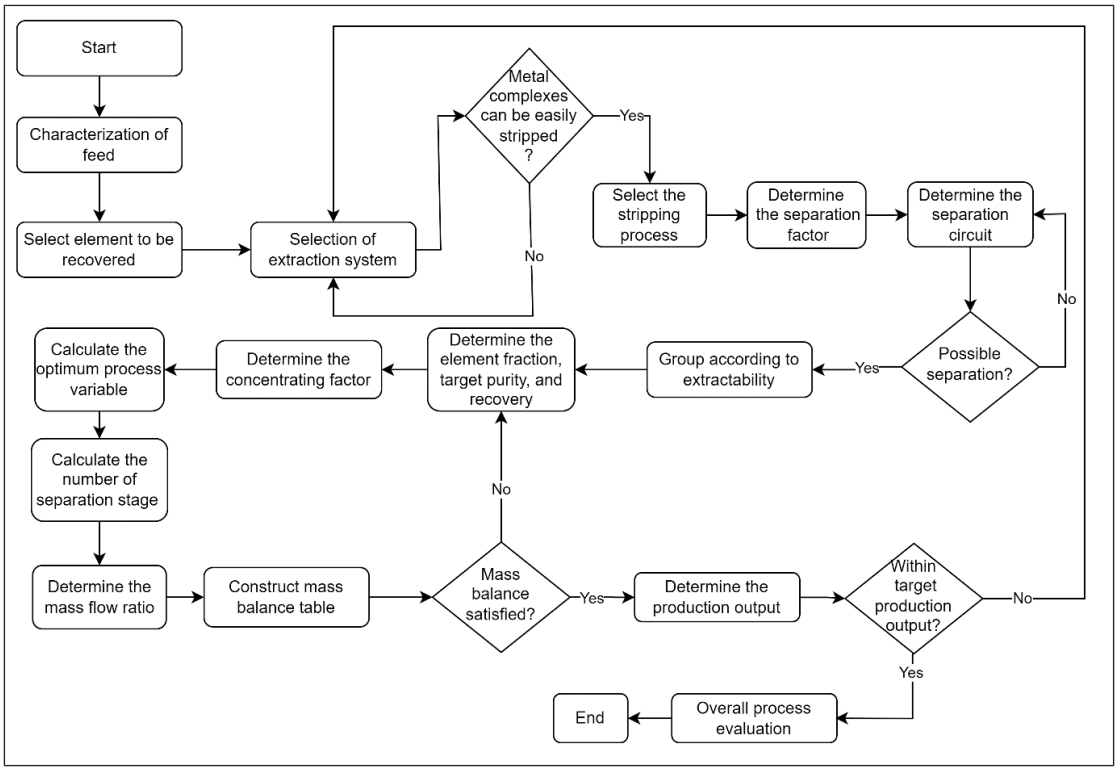

Figure 3: Flowchart outlining the systematic process for designing the REE extraction process.

2.3.1 Framework of methodology

Concentration data of REEs from Malaysian saprolite used in this study were obtained from Tohar and Yunus [4], as depicted in Figure 4. However, it is important to note that this study focused solely on extracting Nd, Pr, Tb, and Dy from these samples, which were assumed to be free from impurities. This assumption is valid because impurities are typically removed effectively through flotation, leaching, precipitation, filtering, and a dedicated low-stage SX circuit before the samples are used as a feed for REE extraction. Considering these factors, it was assumed that the samples were free of contaminants, as it is crucial to emphasize that the samples must be uncontaminated, specifically free from impurities, such as thorium, uranium, iron, and aluminum. The presence of these impurities can result in emulsion formation during the extraction and stripping stages [9].

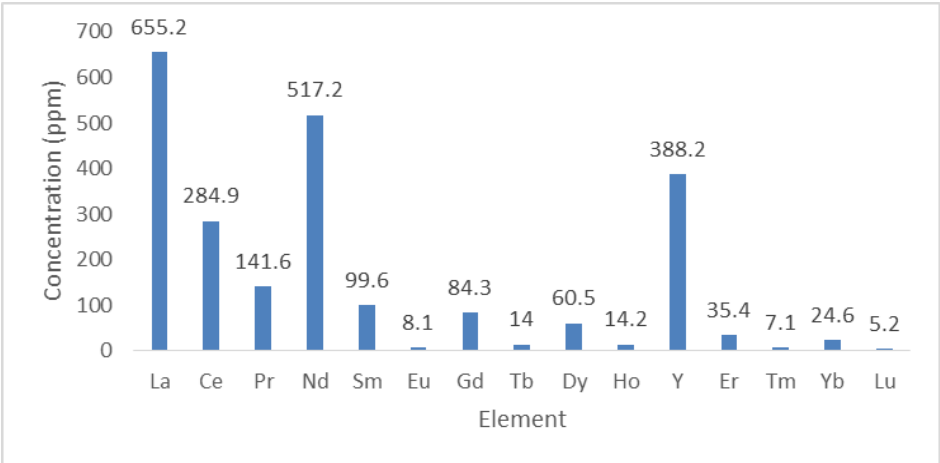

Figure 4: REEs' concentration in saprolite.

2.3.2 Selection of the separation system

The P507-HCl and P204-HCl extraction systems were selected for this study based on their high rankings and suitability for extracting the targeted elements. Cyanex 923 and Cyanex 272 were excluded due to their higher cost and toxicity. Selection of a suitable extraction system is crucial because an unsuitable extractant can form highly stable complexes with rare earth elements that hinder their removal from the extractant. Several factors should be carefully considered when selecting an extraction system. Key attributes that indicate effective extraction include the system's capability to extract the desired elements, selectivity of the extractant for these elements, tendency to form emulsions, loading capacity, ease of stripping, cost of the extractant, and toxicity. It is important to note that each extraction system has its limitations, as no single system can efficiently extract all REEs. Table 2 provides an overview of various extraction systems' attributes, including P507, P204, naphthenic acid, P350 (Di-(1-methylheptyl) methyl-phosphonate), Cyanex 923, and Cyanex 272, thus highlighting their strengths and weaknesses as identified through literature reviews [1,2,10–15].

Table 2: Attributes of rare earth elements in SX systems.

Extraction system	Element	Selectivity	Tendency to form an emulsion	Loading capacity	Stripping difficulty	Cost	Toxicity	Rank
P507	Y, Tb, Dy, Ho, Er	3	3	4	3	3	1	1
P204	La, Ce, Pr, Nd, Sm, Eu, Gd, Sc	2	2	3	3	3	1	2
Naphthenic Acid	Sm, Eu, Gd, Y, Tb, Dy, Ho, Er, Tm, Yb, Lu	1	3	3	4	4	1	3
P350	La, Ce, Pr, Nd, Sm, Tb, Yb, Sc	3	3	1	3	2	1	4
Cyanex 923	La, Ce, Nd, Pr, Sm, Gd, Dy,Yb	2	3	1	2	1	2	5
Cyanex 272	Y, Tm, Yb, Lu	1	3	1	1	2	3	6

*Scoring scale 1: Low, 2: Moderate, 3: High, 4: Very high

2.3.3 Selection of stripping agent

The stripping agent was chosen based on its efficiency in stripping REEs from the extractant. There is no general stripping agent that can be used to strip all REEs. This process involved the use of various concentrations of HCl, HNO_3, and H_2SO_4 to strip off the REEs from the extractant. Selecting the most suitable highly efficient stripping agent is crucial for ensuring that a very high percentage of REEs can be recovered in an aqueous solution, and the extractant can be raffinated back to the extraction and scrubbing stages. The stripping efficiency (S%) was calculated using Eq. (1)[1,2].

$$S\% = \frac{[M^{3+}]^e{}_a}{[M^{3+}]^i{}_o} \times 100 \quad (1)$$

The stripping agent was selected based on the ability of the stripping solution to extract the RE from the organic solution. A stripping agent with a high stripping efficiency is desired because this type of agent requires a smaller number of stripping stages. Table 3 shows the stripping solutions proposed for each element to be extracted and their stripping efficiency (S %).

Table 3: Proposed stripping agents and their stripping efficiency.

Element	Stripping %	Stripping solution	Reference
Nd	99.9	3.0M HCl	[16]
Pr	99.9	3.0M HCl	[17]
Tb	79.0	4.0M HCl	[18]
Dy	81.3	0.1 HNO_3	[19]

2.3.4 Determining the average separation factor

Data for equilibrium distribution ratio (D) and separation factors ($\beta_{z+1/z}$), as shown in Table 4, Table 5, and Table 6, were obtained from published literature sources [1]. The separation path was formulated using the $\beta_{z+1/z}$ data [1,2]

$$D = \frac{[M^{3+}]^e{}_o}{[M^{3+}]^e{}_a} \quad (2)$$

$$\beta_{Z+1/Z} = \frac{D_{Z+1}}{D_Z} \quad (3)$$

Table 4: Distribution ratio data for RE extraction in P507-kerosene-HCl system.

Kinetic Data	REE	Equilibrium	REE	Equilibrium	REE	Equilibrium
[RE], mol/L	La	0.0171	Eu	0.0159	Er	0.0119
D		0.146		0.343		0.740
[RE], mol/L	Ce	0.0179	Gd	0.0160	Tm	0.0114
D		0.159		0.370		0.792
[RE], mol/L	Pr	0.0174	Tb	0.0147	Yb	0.0096
D		0.163		0.492		0.988
[RE], mol/L	Nd	0.0172	Dy	0.0124	Lu	0.0095
D		0.179		0.619		1.025
[RE], mol/L	Sm	0.0154	Ho	0.0114	Y	0.0126
D		0.315		0.729		0.660

Table 5: Separation factor ($\beta_{Z+1/Z}$) P507-HCl-Kerosene at 25 °C, with a P507 concentration of 0.20 mol/L and pH 3.0.

$\beta_{Z+1/Z}$	Ce	Pr	Nd	Sm	Eu	Gd	Tb	Dy	Ho	Er	Tm	Yb	Lu	Y
La	1.09	1.12	1.23	2.16	2.35	2.53	3.37	4.24	4.99	5.07	5.42	6.77	7.02	4.52
Ce	0.00	1.03	1.13	1.98	2.16	2.33	3.09	3.89	4.58	4.65	4.98	6.21	6.45	4.15
Pr		0.00	1.10	1.93	2.10	2.27	3.02	3.80	4.47	4.54	4.86	6.06	6.29	4.05
Nd			0.00	1.76	1.92	2.07	2.75	3.46	4.07	4.13	4.42	5.52	5.73	3.69
Sm				0.00	1.09	1.17	1.56	1.97	2.31	2.35	2.51	3.14	3.25	2.10
Eu					0.00	1.08	1.43	1.80	2.13	2.16	2.31	2.88	2.99	1.92
Gd						0.00	1.33	1.67	1.97	2.00	2.14	2.67	2.77	1.78
Tb							0.00	1.26	1.48	1.50	1.61	2.01	2.08	1.34
Dy								0.00	1.18	1.20	1.28	1.60	1.66	1.07
Ho									0.00	1.02	1.09	1.36	1.41	0.91
Er										0.00	1.07	1.34	1.39	0.89
Tm											0.00	1.25	1.29	0.83
Yb												0.00	1.04	0.67
Lu													0.00	0.64

Table 6: Separation factor P204-HCl-Kerosene at 25 °C with a P204 concentration of 0.30 mol/L and pH 2.78.

$\beta_{Z+1/Z}$	Ce	Pr	Nd
La	2.17	2.07	3.99
Ce	-	0.95	1.84
Pr	-	-	1.93

This study's separation circuit designs were based on the concept of art versus science. This concept involves recovering elements along a specific path rather than extracting individual elements separately each time [20,21]. The concept is implemented by dividing the broad REE spectrum into smaller groups because extracting elements this way is easier and more efficient than attempting to extract each element individually. Figure 5 illustrates the comparison between the scientific method and the "art versus science" method. This serves as the foundation for designing and analysing extraction circuits. According to this concept, elements are grouped and their separation factors are determined as averages rather than individual values. Initially, the elements are grouped based on their extractability. A group of multiple elements must consist of adjacent elements and cannot be non-adjacent. According to Xu's counter-current principle, the purity of easily extractable and difficult solutes will always be at the organic and aqueous outlets respectively. The easily extractable and difficult solutes are assigned to notions *A* and *B,* and these notions can represent either a single REE or a composition of multiple REEs. *A* can be a group of La, Ce, Nd, and Pr, meanwhile, whereas *B* can be the remaining spectrums including Sm, Eu, Gd, Tb, Dy, Ho, Er, Tm, Yb, Lu, and Y. As these elements were treated as a collective group, while acting similarly to an individual element, it was appropriate to introduce the average separation factor (β_{Avg}).

The calculation of β_{Avg} for each circuit is as follows:

$$\beta_{Avg} = \frac{\sum \beta_i}{n_i - 1} \quad (4)$$

Table 7 is used to assist in calculating the average separation factors. The individual average for each element is obtained by summing the separation factor values for that element and dividing them by the number of elements in the row minus one. For example, the average separation factor for La is calculated as (0 + 2.17 + 2.07 + 3.99) ÷ (4 − 1) = 2.74. Once the individual average separation factors are determined (La: 2.74, Ce: 1.653, Pr: 1.650, Nd: 2.59), the group averages for LaCe and PrNd can be calculated by averaging the respective individual values.

Table 7: Summary of data used to calculate average separation factors.

Separation factor ($\beta_{Z+1/Z}$) P507-HCl-Kerosene				
β	La	Ce	Pr	Nd
La	0	2.17	2.07	3.99
Ce	2.17	0.00	0.95	1.84
Pr	2.07	0.95	0.00	1.93
Nd	3.99	1.84	1.93	0.00
Average separation factor (β_{Avg})				
	La	Ce	Pr	Nd
Step 1	2.74	1.653	1.650	2.59
LaCe/NdPr	2.20		2.12	

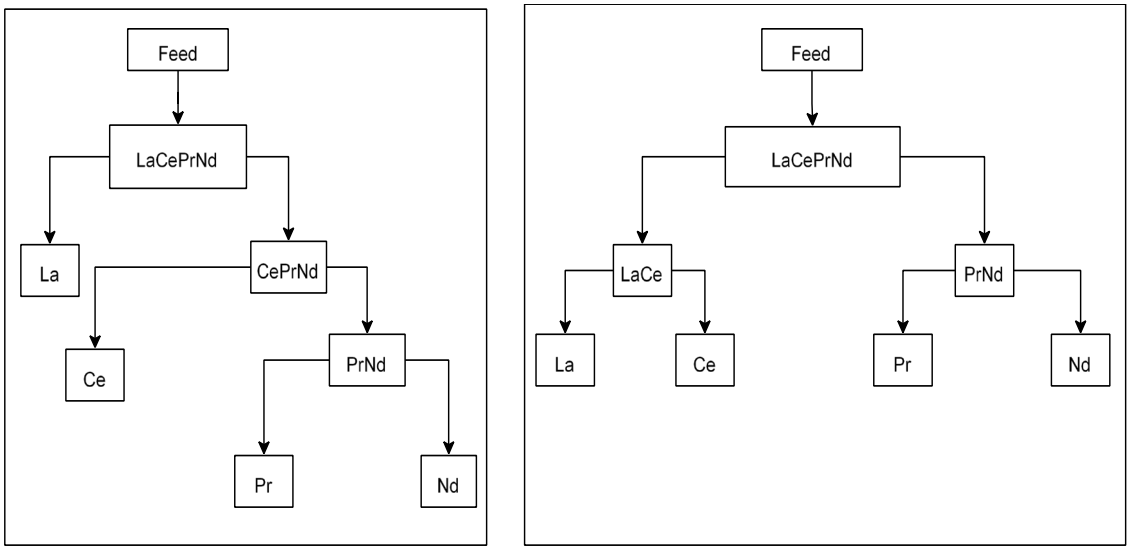

Figure 5: Conceptual illustration of the "art versus science" approach, where rare earth elements are first extracted by group and then separated individually.

2.3.5 Group according to extractability

The large spectrum of REEs was separated into a smaller group of adjacent elements by applying the Art versus Science concept, then their β_{Avg} was determined accordingly. A group of multiple elements must consist of adjacent elements and cannot be non-adjacent. When extracting two adjacent REEs that have the same β_{Avg} value, the *A* and *B* are determined according to the positive sequence. The extraction order of REEs by P204-HCl in kerosene media follows a positive sequence, as in La < Ce < Pr < Nd < Sm < Eu < Gd < Tb < Dy < Ho < Y< Er < Tm < Yb < Lu [22]. While for P507-HCl in kerosene media, the positive sequence, as in La < Ce < Pr < Nd < Sm < Eu < Gd < Tb < Dy < Ho< Er < Tm < Yb < Lu< Y [22]. When extracting La and Ce by using P204-HCl, it has the same β_{Avg} value, while La and Ce are *B* and *A*, respectively. Table 8 shows the β_{Avg} data for REEs according to the extraction system.

Table 8: Circuit extractability.

Step	SX components	Extraction System	
		P204	**P507**
	Separation Factor	β_{Avg}	β_{Avg}
1	LREE/MREE+HREE	n. a	3.38
1(a)	LaCe/NdPr	2.20	n. a
1(b)	Nd/Pr	1.93	n. a
2	MREEs/HREEs	n. a	1.96
3	Tb-Er/Ho-Y	n. a	1.33
3(a)	TbDy/HoEr	n. a	1.31
3(b)	Tb/Dy	n. a	1.26

2.3.6 Calculating the optimum process variable

A set of parameters needs to be determined to acquire an optimum recovery. The most critical parameters are the maximum amount of extraction in the extraction section (S_o) and the scrubbing section (W_a). The type of feeding system (aqueous or organic), cascade section control type (cascade extraction-controlled or cascade scrubbing-controlled), maximum extraction for the solute in extraction (E_M), and scrubbing (E'_M) should be solved first before the values of S_o and W_a can be determined. Figure 6 shows the material balance in the aqueous and organic feeding systems, respectively [1].

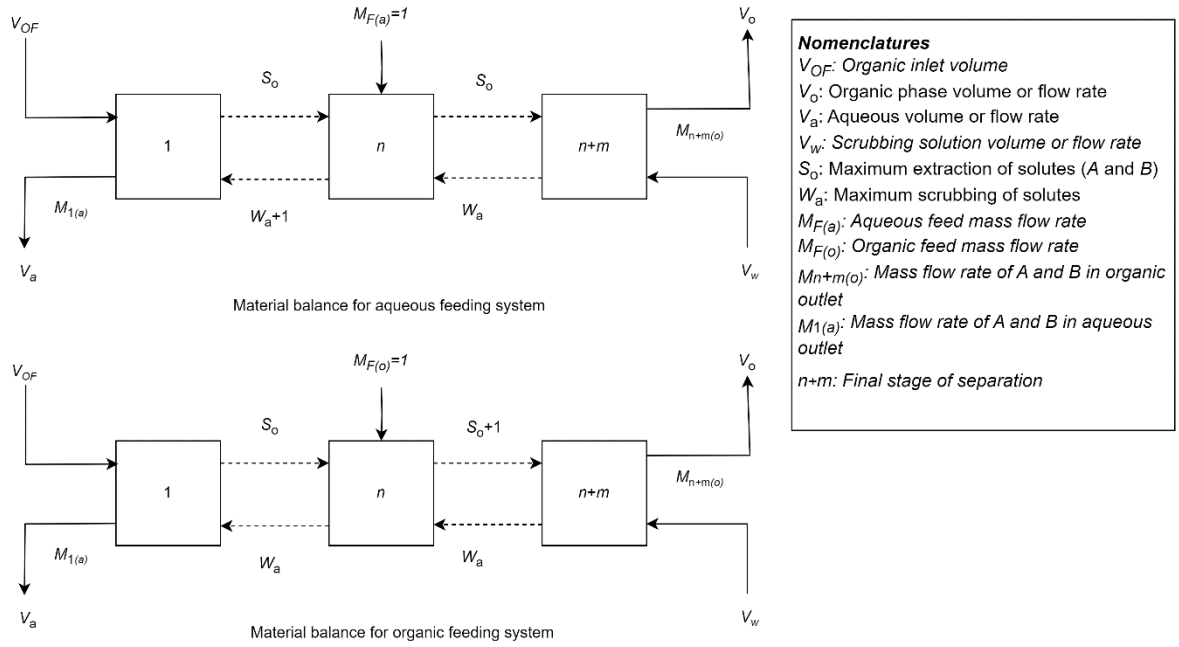

Figure 6: Material balance of the organic and aqueous feeding systems.

At the initial stage of cascade SX, the feed is always the aqueous phase because it is easier to prepare aqueous feed, and in the following stage, *A* is the organic phase feed, and the raffinate *B* is in the aqueous phase feed. Since the separation process comprises extraction and scrubbing sections, it is crucial to identify which section controls the separation process. Cascade extraction-controlled and cascade scrubbing-controlled processes are conditions where the extraction section and scrubbing section control the cascade extraction process, respectively. When the extraction reflux (J_S) is larger than the scrubbing reflux (J_W), the process is cascade extraction

controlled and when (J_S) is smaller than scrubbing reflux (J_W), the process is cascade scrubbing extraction controlled. In the aqueous feeding system, the cascade section control types were determined by Eq. (5) and Eq. (6) [2] and for the organic feeding system, they were determined by Eq. (7) and Eq. (8)[2].

Cascade extraction controlled if $J_S > J_W = f'_B > \frac{\sqrt{\beta}}{(\sqrt{\beta}+1)}$ (5)

Cascade scrubbing controlled if $J_S < J_W = f'_B < \frac{\sqrt{\beta}}{(\sqrt{\beta}+1)}$ (6)

Cascade extraction controlled if $J_S > J_W = f'_B > \frac{1}{(\sqrt{\beta}+1)}$ (7)

Cascade scrubbing controlled if $J_S < J_W = f'_B < \frac{1}{(\sqrt{\beta}+1)}$ (8)

Once the cascade section control type is determined, the maximum extraction of the solute in both extraction (E_M) and scrubbing (E'_M) can be calculated. As for an aqueous feeding system under cascade extraction control, E_M and E'_M were determined using Eq. (9) and Eq. (10), respectively [1], whereas for the cascade scrubbing control, they were determined using Eq. (11) and Eq. (13) [1]. In contrast, for an organic feeding system with cascade extraction control, E_M and E'_M were determined using Eq. (9) and Eq. (13) [1], whereas for an organic feed system with cascade scrubbing control, E_M and E'_M were determined using Eq. (14) and Eq. (13) [1].

$$E_M = \frac{1}{\sqrt{\beta}} \quad (9)$$

$$E'_M = \frac{E'_M f'_B}{E'_M - f'_A} \quad (10)$$

$$E_M = \frac{E'_M f'_A}{E'_M - f'_B} \quad (11)$$

$$E'_M = \frac{1 - E_M f'_A}{f'_B} \quad (12)$$

$$E'_M = \sqrt{\beta} \quad (13)$$

$$E_M = \frac{1 - E'_M f'_B}{f'_A} \quad (14)$$

Once the cascade section control type is identified and the values of E_M and E'_M are known, S_o and W_a can be determined using Eq. (15), Eq. (16), and Eq. (17)[1]. So is calculated consistently across all feeding system types using Eq. (15). However, W_a is determined differently depending on the system, whereby in an aqueous feeding system, W_a is calculated using Eq. (16), while in an organic feeding system, W_a is determined using Eq. (17) [1].

$$S_o = \frac{E_M M_1}{1 - E_M} = \frac{E_M f'_B}{1 - E_M} \quad (15)$$

$$W_a = S_O - M_{n+m(O)} = S_O - f'_A \quad (16)$$

$$W_a = S_O + 1 - M_{n+m(O)} = S_O + 1 - f'_A = S_O + f'_B \quad (17)$$

2.3.7 Calculating the separation stage

Some of the most critical aspects of the SX process are the number of extractions, scrubbing and stripping stages, as well as the flow rate of each phase. It is known that the organic to aqueous phase ratio (O/A ratio) has a very significant effect on the SX process; however, in order to study SX's behaviour from a different unexplored perspective, the O/A ratio was set constant at a ratio of 1:1, where the O/A ratio can be easily adjusted to suit the needs of the process accompanied by new data to obtain the optimized result. Calculations for extraction (n), scrubbing (m), and stripping (S_n) stages were determined according to Xu's counter-current principle [2], as follows:

$$n = logb/logE_A = logb/log\beta E_B \tag{18}$$

$$m = \frac{loga}{\log\left(\frac{1}{E'_B}\right)} - 1 = \frac{loga}{\log\left(\frac{\beta}{E'_A}\right)} - 1 \tag{19}$$

$$S_n = logb/logE_A = logb/log\beta E_B \tag{20}$$

2.3.8 Determine the mass flow ratio and construct the mass balance table

The flow ratio ($V_F/V_o/V_W$) is the ratio of the feed, organic, and scrubbing flow rates, which were determined by using Eq. (21), Eq. (22), and Eq. (23), respectively [1,2]. An assumption made while determining the scrubbing flow rate was that 3.0 mol of *HA* could remove 1.0 mol of RE ions. The mass balance table summarizes all parameters and concentrations of REEs in the aqueous and organic phases throughout the separation stages.

$$V_F = \frac{M_F}{[M_F]} \tag{21}$$

$$V_o = \frac{S_o}{[M_o]} \tag{22}$$

$$V_w = \frac{3W_a}{[HA]} \tag{23}$$

2.4 Overall process evaluation

The aim of the overall process evaluation (OPE) is to determine whether the designated process is operable at an optimum level at all stages, and it can be performed promptly by using the mass balance table. The evaluation is based on the number of separation stages (extraction and scrubbing stages), extraction efficiency, number of stripping stages, stripping efficiency, concentration of feed and scrubbing aqueous solution, concentration of REEs in organic and aqueous phases, mass flow rate, reagent consumption, and phase ratio.

2.4.1 Determine the optimum throughput output

The optimum throughputs of A (Q_A) and B (Q_B) at the organic and aqueous outlets were determined using Eq. (24) and Eq. (25) [1], respectively, where V, t, R, R', $[B_{(1a)}]$, $[A_{(n+m)}]$, and M represent the volume of mixer of each stage, phase ratio of extraction, phase ratio of scrubbing, concentration of B at the aqueous outlet, concentration of A at the organic outlet, and molar mass, respectively. The phase ratio (R *and* R') and concentrations of A ($[A_{(n+m)}]$) and B ($[B_{(1a)}]$) in the organic and aqueous outlets must be determined before the optimum production of A and B can be determined. R and R' were determined according to Eq. (26) to Eq. (27) [1]. $[B_{(1a)}]$ and $[A_{(n+m)}]$

depend on the feeding system, and they were determined according to Eq. (28) to Eq. (31) [1], respectively.

$$Q_{\mathrm{B}} = 1.44 \frac{V}{t} \frac{[B_{1(a)}]}{(1+R)} \tag{24}$$

$$Q_{\mathrm{A}} = 1.44 \frac{V}{t} \frac{[A_{(n+m)}]}{(1+R')} \tag{25}$$

The phase ratio for extraction (R) and scrubbing (R') was determined as follows:

$$R = \frac{V_o}{V_w + V_F} \tag{26}$$

$$R' = \frac{V_o}{V_w} \tag{27}$$

A and B concentrations at organic and aqueous outlets for an aqueous feeding system were determined as follows:

$$[A_{(n+m)}] = \frac{M.f'_A.M_{F(a)}}{V_o} \tag{28}$$

$$[B_{1(a)}] = \frac{M.f'_B.M_{F(a)}}{V_f + V_w} \tag{29}$$

A and B concentrations at organic and aqueous outlets for an organic feeding system were determined as follows:

$$[A_{(n+m)}] = \frac{M.f'_A.M_{F(o)}}{V_o + V_F} \tag{30}$$

$$[B_{1(a)}] = \frac{M.f'_B.M_{F(o)}}{V_W} \tag{31}$$

3. RESULTS AND DISCUSSION

3.1 The selection of the solvent extraction system

Extractants' attribute data were obtained from various literature sources, as detailed in Section 2.0, with the attributes measured in arbitrary units. Figure 7 presents the attributes of P204, P507, P350, Cyanex 272, Cyanex 923, and naphthenic acid extractants. Upon evaluating these extractant properties, it was evident that P507 and P204 were the most effective among the six extractants, considering attributes such as the emulsion formation tendency, loading selectivity, capacity, stripping difficulty, cost, and toxicity. In general, P507 and P204 exhibited superior performance compared with other extractants in terms of their low tendency to form emulsions, selectivity of rare earths, loading capacity, cost-effectiveness, and toxicity levels. However, it is worth noting that these extractants posed a moderate level of difficulty during the stripping processes, which is a drawback when considered.

Figure 7: Attribute analysis of SX extraction systems.

3.2 Separation complexity analysis

As mentioned earlier, the separation data utilized in this study were based on the P507-HCl and P204-HCl systems in a kerosene medium. Table 8 lists the average separation factors (β_{Avg}) of the 15 elements in the P507-HCl. β_{Avg} was calculated by sorting the separation factor ($\beta_{Z+1/Z}$) element versus the elements in the rows and columns. The β_{Avg} for each element was acquired by summing the total $\beta_{Z+1/Z}$ divided by n-1. The β_{Avg} values for each element from which the separation circuits/pathways were formulated are presented in Table 8. As implied by the "Art versus Science" concept, the elements were split into LREEs, MREEs, and HREEs according to their extractability. Using the aforementioned method, the β_{Avg} values for LREEs, MREEs, HREEs, LREEs/MREEs+HREEs, and MREEs/HREEs were calculated based on data from Table 5 and are presented in Table 9.

Table 9: Average separation factor of LREEs, MREEs, and HREEs.

Circuit	β_{Avg}		
	LREE	**MREE**	**HREE**
LREEs/MREEs+HREEs	3.38	2.23	
MREEs/HREEs	Not applicable	1.96	1.55

The approach used for formulating the circuit to extract LREEs and MREEs was also applied to determine the β_{avg} for La, Ce, Nd, Pr, Tb, Dy, Ho, Tm, Yb, Lu, and Y. Table 10 presents the extraction circuit used for La, Ce, Nd, and Pr, along with their corresponding β_{Avg} values calculated from Table 6. Three circuits were required to extract the LaCe/NdPr, La/Ce, and Nd/Pr elements. Five separation circuits were required to recover Tb, Dy, Ho, Er, and Y, as in Tb–Tb-Er/Tm-Y, TbDy/HoEr, Tb/Dy, Ho/Er, and Tm-Lu/Y. The β_{avg} values of these circuits, calculated based on Table 5, are listed in Table 11. Based on the β_{avg} value of each circuit, it was observed that recovering Tb and Dy was more difficult than recovering Nd and Pr because of their lower separation factors. A lower separation factor indicates a lower maximum amount of extraction and higher separation stages.

Table 10: Average separation factor of LREEs.

Circuit	β_{Avg}			
	La	**Ce**	**Nd**	**Pr**
LaCe/NdPr	2.20		2.17	
Nd/Pr	Not applicable		1.93	1.93

Table 11: Average separation factor of HREEs.

Circuit	β_{Avg}							
	Tb	**Dy**	**Ho**	**Er**	**Tm**	**Yb**	**Lu**	**Y**
Tb-Er/Tm-Y	1.30				1.20			
TbDy/HoEr	1.31		1.23		Not applicable			
Tb/Dy	1.26	1.26	Not applicable					

3.3 Process modelling

Process modelling was conducted to assess the recoveries of Nd, Pr, Tb, and Dy. Table 12 lists the overall process parameters required to achieve a recovery rate of at least 99.0% and 99.99% purity. Figure 8 shows the complete process flow for acquiring these elements (circuits). Recovering 99.0% of Nd, Pr, Tb, and Dy products with 99.99% purity required 379 stages of the cascade SX process. The feed mass flow rate in this model was maintained constant at 1.0 mol/L.. *A* was in the pregnant organic solution, and *B* remained in the raffinate. Notably, circuits such as Tb-Er/Tm-Y, Tb-Dy/Ho-Er, and Dy/Tb require longer separation stages due to the low separation factors between heavy rare earth elements. This necessitates numerous extraction stages to achieve high purity, resulting in larger and more complex equipment. Handling large volumes increases residence times and can cause issues like phase mixing. Maintaining consistent phase ratios and flow rates throughout all stages is challenging and requires careful control. Furthermore, larger equipment leads to higher costs and energy consumption, along with increased solvent usage, thus making the process more expensive.

Table 12: Separation modelling data.

Item	**Separation circuit**						
Variable	1 LREEs/ MREEs- HREEs	1(a) LaCe/PrNd	1(b) Pr/Nd	2 MREEs/ HREEs	3 TbEr/ Tm-Y	3(a) TbDy/ HoEr	3(b) Dy/Tb
Feed ratio (%)	68.3/31.7	58.8/41.2	21.5/78.5	74.1/25.9	22.6/77.4	60.1/39.9	81.2/18.8
Purity	99.99	99.99	99.99	99.99	99.99	99.99	99.99
Recovery	99.0	99.0	99.0	99.0	99.0	99.0	99.0
Average separation factor, β_{Avg}	3.38	2.20	1.93	1.96	1.33	1.31	1.26
Feeding System	Aqueous	Aqueous	Aqueous	Aqueous	Aqueous	Organic	Organic
Feed O/A	1:1	1:1	1:1	1:1	1:1	1:1	1:1

Table 12. Continued.

Item	Separation circuit						
Variable	1 LREEs/ MREEs- HREEs	1(a) LaCe/ PrNd	1(b) Pr/ Nd	2 MREEs/ HREEs	3 Tb-Er/ Tm-Y	3(a) TbDy/ HoEr	3(b) Dy/ Tb
Average extraction factor in extraction, E_M	0.82	0.81	0.93	0.71	0.87	0.9	0.97
Average extraction factor in scrubbing, E'_M	1.84	1.48	1.38	1.17	1.05	1.14	1.12
Extraction reflux ratio, J_s	4.59	4.28	12.45	2.50	6.53	9.15	32.5
Scrubbing reflux ratio, J_w	1.19	2.07	2.57	5.88	20.41	6.92	8.16
Maximum extraction of solutes (A and B), S_o	1.48	1.79	2.77	1.83	5.00	3.71	6.37
Feed flow rate, V_F	1.00	1.00	1.00	1.00	1.00	1.00	1.00
Organic flow rate, V_o	1.54	3.46	11.1	7.34	20.00	11.22	6.4
Scrubbing flow rate, V_w	1.21	1.81	2.99	2.35	7.15	6.17	9.85
Effective Phase ratio, R	0.70	1.23	2.78	2.19	2.45	1.56	0.59
Extraction stage, n	6	9	9	25	56	29	24
Scrubbing stages, m	13	22	24	10	20	65	67
Total stage, T	19	31	33	35	76	94	91
Striping O/A	1:1	1:1	1:1	1:1	1:1	1:1	1:1
Stripping stage, S_n	3	Not required	1/1	Not required	Not required	Not required	4/5

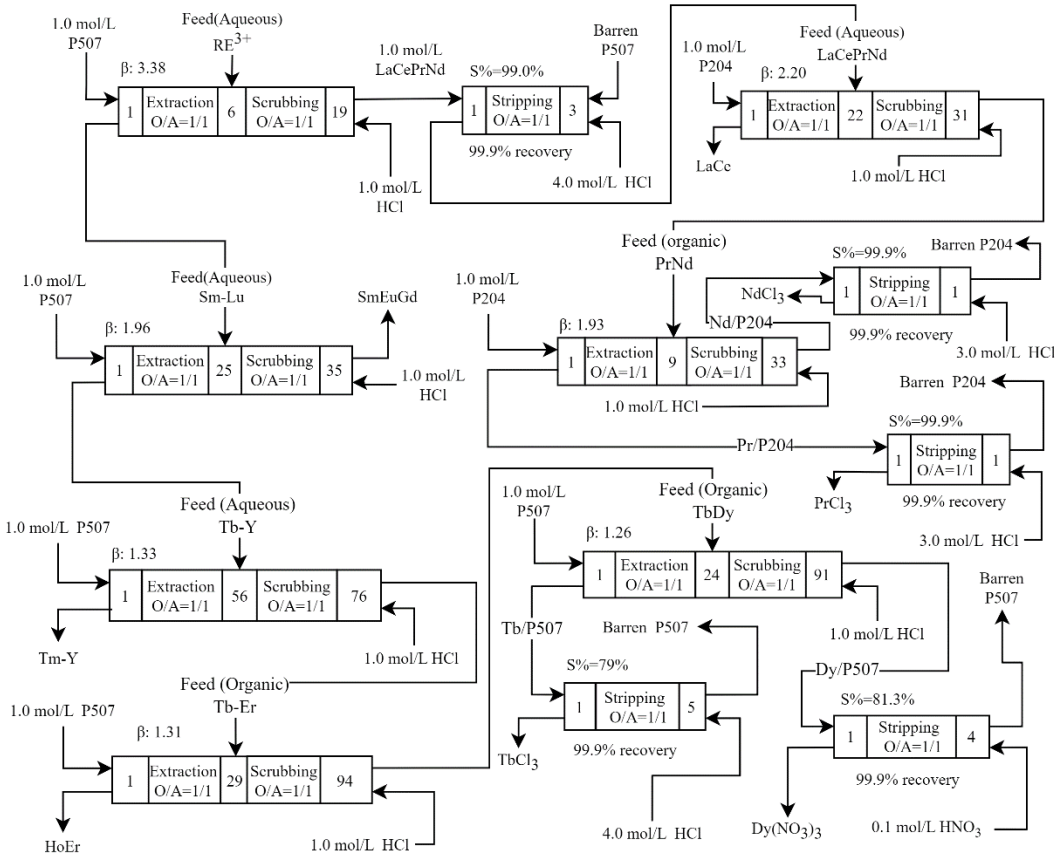

Figure 8: Overall Separation circuit.

3.4 The recovery behaviour of REEs in extraction and scrubbing streams

It was generally observed that the behaviour of the separation and the recovery of large fractions *A* and *B* depends on the type of control mode, which is whether the process is dependent on either extraction or scrubbing control. As for the cascade scrubbing-controlled process, most of the recovery of *A* occurred in the extraction phase, whereas the accumulation of *B* occurred in the scrubbing stage. Meanwhile, if the process is extraction-controlled, most of the recovery of *A* occurred in the scrubbing stage, and the concentration of *B* occurred during the extraction phase. This argument is supported by Figures 9 and 10. The condition is related to the correct working point of separation, whereby the working point is defined as *A* and *B,* both having reached approximately 50% recovery. However, it is impossible to obtain exactly 50% at the working point at any stage due to the variations between fractions of *A* and *B* during the feed section. Hence, the practical working point (which is ideally ≈50% recovery at the extraction stage) can be reconciled and adjusted by the intersection of recovery *A* and *B* at any stage (regardless of whether it is in the extraction or scrubbing phase). The primary purpose of identifying the working point condition is precisely to determine the minimum number of stages that is essential for establishing an effective extraction zone (effective extraction is logical when 50% of the extraction rate occurs) [23].

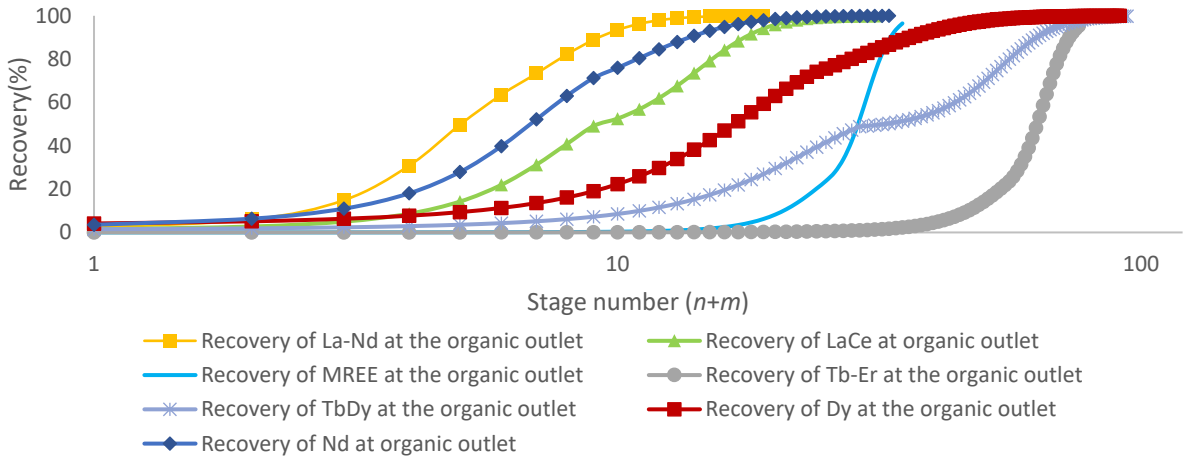

Figure 9: Recovery trends of La-Nd, LaCe, MREE, Tb-Er, TbDy, Dy and Nd at the organic outlets.

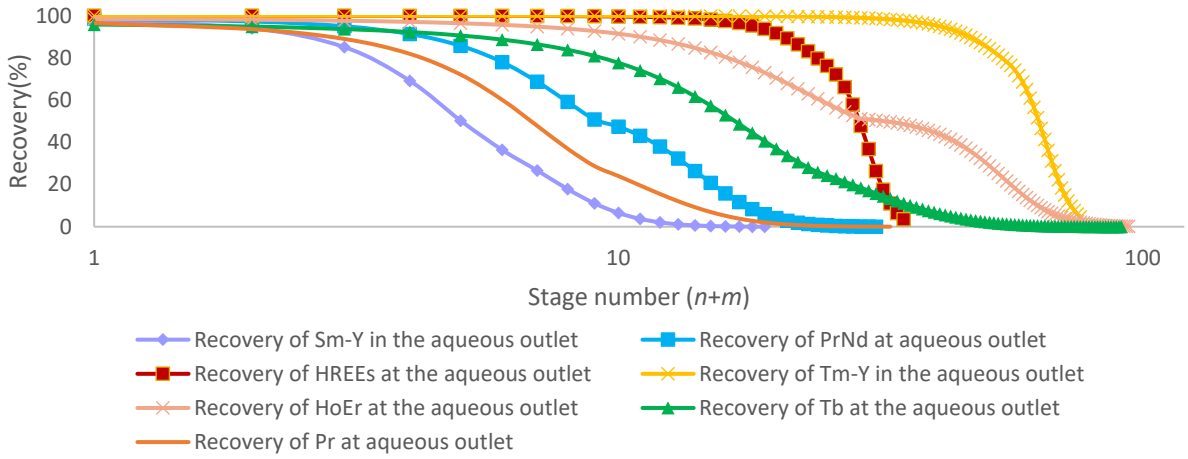

Figure 10: Recovery trends of Sm-Y, PrNd, HREE, Tm-Y, HoEr, Tb and Pr at the aqueous outlets.

3.5 Model validation

Model verification was carried out based on the experimental data of E_M, E'_M, n, and m. The modelling data closely aligned with the experiment data with diminutive variation. The model was verified by a comparison study involving modelling data and actual experimental data, as shown in Table 13 [24]. The comparison between the extraction and scrubbing stages from the experimental and modelling data shows a close match, as depicted in Figures 11 and 12. The modelling results closely approximate the experimental data. The extraction data used in the experiment were also utilized in the model and later helped determine the percentage errors. An error of less than 5% indicates that the results from the model were accurate and reliable. Verification of the model was based on the separation factor (β) at 2, 4, and 8, while the feed fraction was tested at 0.05 until 0.95.

Table 13: Separation modelling data.

β	f_A	$P_{B1(a)}$	$P_{An+m\,(o)}$	**Experimental data**				**Modelling data**			
				E_M	E'_M	n	m	E_M	E'_M	n	m
2.0	0.05	0.9999	0.999	0.707	1.020	18	15	0.707	1.022	18.1	15.6
	0.1	0.9999	0.999	0.707	1.050	21	14	0.707	1.048	20.2	15.5
	0.2	0.9999	0.9999	0.707	1.120	24	19	0.707	1.116	22.6	18.5
	0.4	0.9999	0.9999	0.707	1.380	34	30	0.707	1.381	32.0	28.8
	0.5	0.9999	0.9999	0.773	1.410	26	27	0.773	1.414	25.7	27.2
	0.6	0.9999	0.9999	0.837	1.410	22	24	0.837	1.414	21.1	24.4
	0.8	0.9999	0.9999	0.923	1.410	20	20	0.932	1.414	19.4	21.6
	0.9	0.999	0.9999	0.950	1.410	17	17	0.968	1.414	17.5	15.2
	0.95	0.999	0.9999	0.985	1.410	17	15	0.985	1.414	16.1	15.1
4.0	0.05	0.9999	0.999	0.500	1.060	10	7	0.500	1.057	10.0	7.7
	0.1	0.9999	0.999	0.500	1.130	11	7	0.500	1.126	11.1	7.5
	0.2	0.9999	0.9999	0.500	1.330	13	9	0.500	1.335	12.6	10.6
	0.4	0.9999	0.9999	0.571	2.000	14	14	0.572	0.200	14.6	14.8
	0.5	0.9999	0.9999	0.667	2.000	12	12	0.6667	2.000	12.6	13.2
	0.6	0.9999	0.9999	0.750	2.000	11	11	0.750	2.000	11.4	11.7
	0.8	0.9999	0.9999	0.889	2.000	11	9	0.889	2.000	9.3	10.3
	0.9	0.999	0.9999	0.947	2.000	9	8	0.947	2.000	8.8	9.1
	0.95	0.999	0.9999	0.974	2.000	10	7	0.974	2.000	8.5	8.0
8.0	0.05	0.9999	0.999	0.354	1.110	7	5	0.354	1.106	6.03	4.65
	0.1	0.9999	0.999	0.354	1.250	8	4	0.354	1.255	6.75	3.73
	0.2	0.9999	0.9999	0.354	1.840	10	7	0.354	1.843	9.74	6.27
	0.4	0.9999	0.9999	0.508	2.830	9	8	0.508	2.828	7.92	8.86
	0.5	0.9999	0.9999	0.607	2.830	8	7	0.699	2.828	7.6	7.5
	0.6	0.9999	0.9999	0.699	2.830	8	7	0.607	2.828	8.2	8.4
	0.8	0.9999	0.9999	0.861	2.830	8	6	0.861	2.828	7.4	6.5
	0.9	0.999	0.9999	0.993	2.830	7	5	0.933	2.828	7.0	5.7
	0.95	0.999	0.9999	0.967	2.830	7	4	0.967	2.828	6.8	5.0

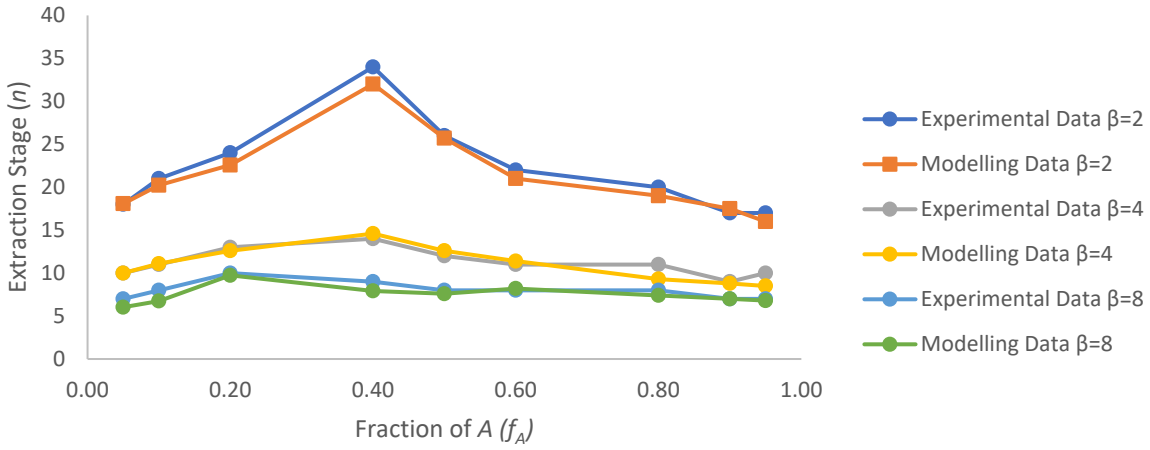

Figure 11: Comparison of extraction stages: experimental vs. modelling data.

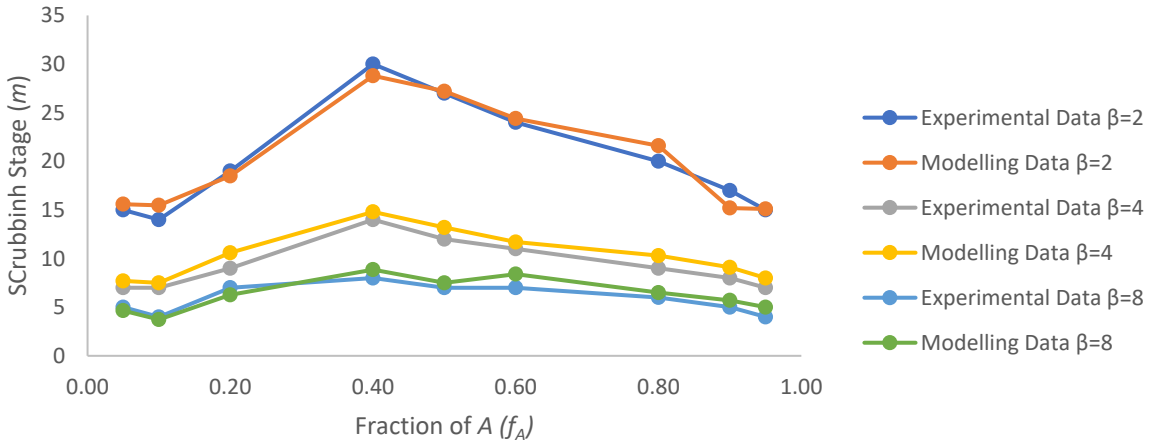

Figure 12: Comparison of scrubbing stages: experimental vs. modelling data.

3.6 The effect of the average separation factor and ratio A/B on the separation stage

The correlation between the average separation factor (β_{Avg}) and the ratio of A to B was significant and influenced the number of separation stages. Figure 13 shows the relationship between β_{Avg} and the A/B ratio in the separation stage.

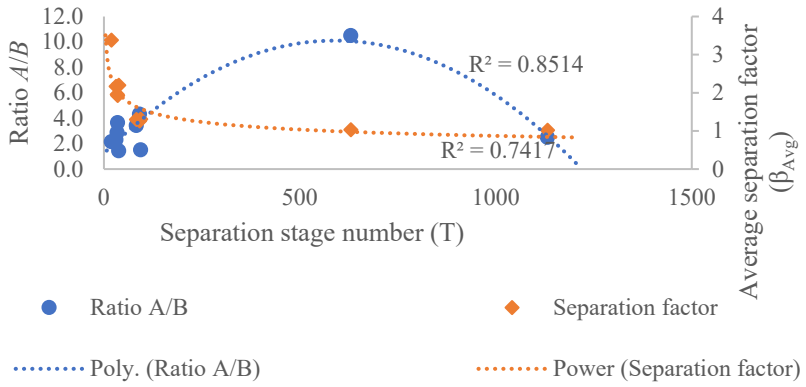

Figure 13: Graph of the average separation factor and ratio A to B versus the total separation stage.

The trend line for β_{Avg} shows that it initially had a significant influence on the number of separation stages, but its impact diminished over time. The A/B ratio shows that an increase in the A/B ratio increases the number of separation stages. At a certain point, when the separation factor decreased, the A/B ratio did not significantly affect the separation stage. Based on the trendline projection, the ideal A/B ratio was approximately 50% for A and B. This indicates that the A/B ratio is a dependent variable rather than an independent variable. The R-squared values for ratios A/B and β_{Avg} are 0.8514 and 0.7417, respectively, which indicate data variation fit in the models. The proposed model can be used to predict the optimum A/B ratio for a particular β_{Avg}.

3.7 The effect of extraction reflux and scrubbing reflux ratios on the separation stages

The relationship between extraction reflux (J_s) and scrubbing reflux (J_W) to separation stage number (T) is illustrated in Figure 14. The graph indicates that low J_s and J_W values are preferred because a high amount of reflux changes the feed composition. Thus, if there are larger differences in the compositions of A and B, it is expected that the separation would become more difficult. This was supported by the model discussed above, which stated that the ideal composition of A to B (or ratio A/B) was 50%/50%, and the R-squared values for the J_W and J_s trend lines were 0.9728 and 0.9992, respectively, indicating that the data are consistent with the proposed model.

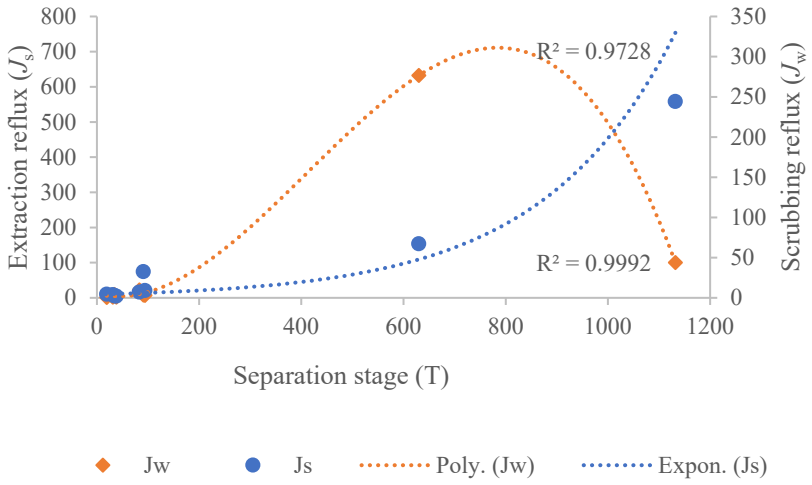

Figure 14: Variation of extraction reflux (J_s) and scrubbing reflux (J_w) with total separation stages (T).

3.8 Optimized throughput

The key criterion for effective rare earth extraction is that the process must be capable of simultaneously producing high-purity products, high product recovery, and high throughput. A high throughput is crucial because it indicates a lower production cost for the separation process. It is cost-ineffective if the process can produce high purity and recovery, but lower output. Optimum production output was achieved by utilizing the optimum parameters discussed previously. The separation was achieved using a series of mixer-settler batteries, where the same size of the mixer settler was used at a 1.40 volume ratio of mixer to settler (r) for each separation circuit, and the mixing time was five minutes. Table 14 lists the constant variables for the model, and Table 15 lists the optimized production outputs of the extracted elements. Assuming that 80% of the processing units were utilized for annual production, the annual productions of Pr, Nd, Tb, and Dy were 20.18 Mg, 25.95 Mg, 3.75 Mg, and 5.86 Mg, respectively.

Table 14: Constant process parameters.

Constant variable	Mass flow rate in the aqueous outlet	Organic concentration, [M_o] (mol/ dm^3)	Scrubbing acid concentration, *HA* (mol/ dm^3)	Feed flow rate, V_F (cm^3/min)	Volume ratio of mixer to settler, *r* (dm^3)	Contact time, *t* (min)
Data	1.00	0.25	2.00	1.00	1.40	5.0

Table 15: Optimized process parameters and throughput.

Variable	Element			
	Pr	Nd	Tb	Dy
Extractability	*B*	*A*	*B*	*A*
Organic flow rate, V_o (cm^3/min)	11.096	11.096	25.472	25.472
Scrubbing flow rate, V_w (cm^3/min)	2.995	2.995	9.846	9.846
Separation Stage number (*T*)	33	33	91	91
Stripping stage (S_n)	1	1	4	5
Concentration of *A* in organic outlet [$A_{(n+m)}$]	-	10.10	-	4.94
Conc.of *B* in aqueous outlet, [$B_{1(a)}$] (g/dm^3)	7.86	-	3.16	-
Phase ratio, *R*	2.78	2.18	2.35	2.35
Daily output (kg/day)	69.12	88.88	12.85	20.06
Annual Production (Mg)	20.18	25.95	3.75	5.86
Total Production (Mg)	55.74			

4. CONCLUSIONS

The proposed framework offers conceptual clarity and a systematic approach to planning REE extraction using multiple extraction systems. Although the practical implementation can be complex, particularly due to the large number of separation stages, the structured methodology helps simplify the overall process design and evaluation. This framework has been applied to design processes specifically targeting the extraction of Pr, Nd, Tb, and Dy from saprolite. The framework addresses material balance, throughput considerations, and operational performance evaluation for the entire SX process. In addition, the optimization extraction parameters were integrated into the framework to simplify the process design. The extraction process required 379 separation stages to achieve 99.99% purity and 99.0% recovery of Pr, Nd, Tb, and Dy. Notably, the ratio of the *A* to *B* feed fraction and the reflux ratio were significantly correlated with the number of separation stages required. This indicates that variations in these parameters have a significant impact on the overall separation efficiency and directly influence the design and complexity of the extraction process. These parameters play a crucial role in optimizing the extraction process and ensuring high purity and recovery rates of the targeted REEs. A multi-extraction system modelling requires a separation of data, which is not readily available. One of the main challenges in modelling multi-extraction systems is the lack of detailed, system-specific extraction data. In order to address this issue, future studies should focus on building a comprehensive data library through systematic experimental studies covering all commonly used extraction systems.

NOMENCLATURES

$[M_{(a)}]$	The total concentration of rare earth in the aqueous phase, mol/dm^3
$[M_o]$	The total concentration of rare earth in the organic phase, mol/dm^3
A	Solute(s) easily extractable
a	The concentrating factor of a
$A_{(n+m)}$	Concentration of A in the organic outlet
b	The concentrating factor of B
B	Solute(s) difficult to extract
$B_{1(a)}$	Concentration of B in aqueous outlet
D	Distribution coefficient
E'_M	Average extraction factor in scrubbing
E_A	Average extraction factor of A in the extraction
E_B	Average extraction factor of B in the extraction
E_M	Average extraction factor in the extraction
f'_A	Mole fraction of solutes (A+B) in organic outlet
f'_B	Mole fraction of solutes (A+B) in aqueous outlet
f_A	Mole fraction of A in feed
f_B	Mole fraction of B in feed
HA	Acid concentration in the scrubbing solution, mol/dm^3
J_S	Extraction reflux ratio
J_W	Scrubbing reflux ratio
m	Number of scrubbing stages excluding the feeding stage
$M_{(a)}$	The mass flow rate of an aqueous phase, mol/min
$M_{(o)}$	The mass flow rate of the organic phase, mol/min
$M_{n+m(o)}$	The mass flow rate of A and B in the organic outlet
n	Number of extraction stages, including the feeding stage
$P_{An+m\ (o)}$	Purity at the final organic outlet
$P_{B1(a)}$	Purity at the final aqueous outlet
Q_A	optimum throughputs of A at the organic outlet
Q_B	optimum throughputs of B at the aqueous outlet
r	Volume ratio of mixer to settler
R	Phase ratio of extraction
R'	Phase ratio of scrubbing
S%	Stripping efficiency
S_n	Number of stripping stages
S_o	Maximum extraction of solutes (A and B), mmol/min
t	Time, min
T	Total stage number of extraction stage and scrubbing
V_F	Feed flow rate, cm^3/min
V_O	Organic flow rate, cm^3/min
V_w	Scrubbing flow rate, cm^3/min
$W_{(a)}$	Maximum scrubbing of solutes, mmol/min
$\beta_{(Z+1/Z)}$	Adjacent separation factor in extraction
$\beta'_{(Z+1/Z)}$	Adjacent separation factor in scrubbing
β'_{Avg}	Average separation factor in scrubbing
β_{Avg}	Average separation factor in extraction

ABBREVIATIONS

HREE	Heavy Rare Earth Element
LREE	Light Rare Earth Element
MREE	Middle Rare Earth Element
OPE	Overall Process Evaluation
REE	Rare Earth Elements
SX	Solvent Extraction

ACKNOWLEDGMENT

This research was funded by the Research and Innovation Department, Universiti Malaysia Pahang Al-Sultan Abdullah, Malaysia (Flagship UMP grant No. PDU213003-3).

REFERENCES

[1] Zhang, J., Zhao, B., & Schreiner, B. *Separation Hydrometallurgy of Rare Earth*. Springer (2016).
[2] Dezhi, Q. *Hydrometallurgy of Rare Earths: Extraction and Separation*. Elsevier (2018).
[3] The Academy of Sciences Malaysia. *Sustainable mining: Rare earth industries*. The Academy of Sciences Malaysia (2019).
[4] Tohar, S. Z., & Yunus, M. Y. M. Mineralogy and BCR sequential leaching of ion-adsorption type REE: A novelty study at Johor, Malaysia. *Physics and Chemistry of the Earth*, vol 120 (2020) p. 102947.
[5] Hamzah, Z., Ahmad, N. M., & Saat, A. Determination of heavy minerals in "Amang" from Kampung Gajah ex-mining area. *Malaysian Journal of Analytical Sciences*, vol 13 (2009) pp. 194–203.
[6] Van Gosen, B. S., & Lowers, H. A. Iron Hill (Powderhorn) carbonatite complex, Gunnison County, CO - a potential source of several uncommon mineral resources. *Mining Engineering*, vol 59 (2007) pp. 56–62.
[7] Van Gosen, B. S., Verplanck, P. L., Seal II, R. R., Long, K. R., & Gambogi, J. *Critical mineral resources of the United States— Economic and environmental geology and prospects for future supply*. U.S. Geological Survey Professional Paper 1802 (2017) pp. O1-O31.
[8] Long, K. R., Van Gosen, B. S., Foley, N. K., & Cordier, D. The principal rare earth elements deposits of the United States: A summary of domestic deposits and a global perspective. In: *Non-Renewable Resources: Issues in Geosciences and Society's Challenges* (2012) pp. 131–155.
[9] Wu, W., Li, D., Zhao, Z., Chen, J., Zhang, F., & Yin, S. Formation mechanism of micro emulsion on aluminum and lanthanum extraction in P507-HCl system. *Journal of Rare Earths*, vol 28 (2010) pp. 174–178.
[10] Duan, T., Li, H., Kang, J., & Chen, H. Cyanex 923 as the extractant in a rare earth element impurity analysis of high-purity cerium oxide. *Analytical Sciences*, vol 20 (2004) pp. 921–924.
[11] Zhang, W., Feng, D., Xie, X., Tong, X., Du, Y., & Cao, Y. Solvent extraction and separation of light rare earths from chloride media using HDEHP-P350 system. *Journal of Rare Earths*, vol 40 (2022) pp. 328–337.
[12] Liao, C. F., Jiao, Y. F., Liang, Y., Jiang, P. G., & Nie, H. P. Adsorption-extraction mechanism of heavy rare earth by Cyanex272-P507 impregnated resin. *Transactions of Nonferrous Metals Society of China (English Edition)*, vol 20 (2010) pp. 1511–1516.
[13] Peelman, S., Kooijman, D., Sietsma, J., & Yang, Y. Hydrometallurgical recovery of rare earth elements from mine tailings and WEEE. *Journal of Sustainable Metallurgy*, vol 4 (2018) pp. 367–377.

[14] Gergoric, M., Barrier, A., & Retegan, T. Recovery of rare-earth elements from Neodymium magnet waste using glycolic, maleic, and ascorbic acids followed by solvent extraction. *Journal of Sustainable Metallurgy*, vol 5 (2019) pp. 85–96.
[15] Regad, M., & Binnemans, K. E. B. M. O. A. Separation of rare earths by mixtures of an ionic liquid and a neutral extractant. *2nd Conference on European Rare Earth Resources* (2017).
[16] Sun, P. P., Seo, H., & Cho, S. Y. Recovery of neodymium, dysprosium, and iron from spent mobile phone camera module magnets through a hydrometallurgical method. *Minerals Engineering*, vol 163 (2021).
[17] Liu, Y., Jeon, H. S., & Lee, M. S. Solvent extraction of Pr and Nd from chloride solution by the mixtures of Cyanex 272 and amine extractants. *Hydrometallurgy*, vol 150 (2014) pp. 61–67.
[18] Gijsemans, L., Forte, F., Onghena, B., & Binnemans, K. Recovery of rare earths from the green lamp phosphor LaPO4:Ce3+,Tb3+ (LAP) by dissolution in concentrated methanesulphonic acid. *RSC Advances*, vol 8 (2018) pp. 26349–26355.
[19] Chen, W. S., Jian, G. C., & Lee, C. H. Recovery and separation of Dysprosium from waste Neodymium magnets through Cyphos IL 104 extraction. *Materials (Basel)*, vol 15 (2022).
[20] Yusri, M., Yunus, M., Ismail, A., & Abdul, B. *Introduction to Separation Index: Modelling of Rare Earth Element Extraction Complexity for Feasible Processing* (2016).
[21] Mackowski, S. *Mackowski.pdf* (2014).
[22] Wang, C., Yan, R., Cui, H., Shi, J., Yan, N., & You, S. Separation of yttrium from ion-adsorbed-rare-earth deposit leachates using N,N-di(2-ethylhexyl)-diglycolamic acid (HDEHDGA): Preliminary experimental and molecular dynamics simulation studies. *Hydrometallurgy*, vol 231 (2025).
[23] Talens Peiró, L., & Villalba Méndez, G. Material and energy requirement for rare earth production. *JOM*, vol 65 (2013) pp. 1327–1340.
[24] Li, B., Y., N., & Xu, G. *Theory of countercurrent extraction volume V (in Chinese)* (1982).

Conflicts of interest statement: The authors declare that there is no conflict of interest.

Author contributions statement: Conceptualization, Farouq, and Mohd Yusri; Methodology, Farouq; Modelling, Farouq, and Mohd Yusri; Investigation, Farouq; Resources, Mohd Yusri; Data Curation, Farouq; Writing – Original Draft Preparation, Farouq; Writing – Review & Editing, Mohd Yusri; Visualization, Farouq; Supervision, Mohd Yusri.